

# All Weight Systems for Calabi–Yau Fourfolds from Reflexive Polyhedra

Friedrich Schöller<sup>\*</sup> and Harald Skarke<sup>†</sup>

Institut für Theoretische Physik, Technische Universität Wien  
Wiedner Hauptstraße 8–10, 1040 Wien, Austria

## ABSTRACT

For any given dimension  $d$ , all reflexive  $d$ -polytopes can be found (in principle) as subpolytopes of a number of maximal polyhedra that are defined in terms of  $(d + 1)$ -tuples of integers (weights), or combinations of  $k$ -tuples of weights with  $k < d + 1$ . We present the results of a complete classification of sextuples of weights pertaining to the construction of all reflexive polytopes in five dimensions. We find 322 383 760 930 such weight systems. 185 269 499 015 of them give rise directly to reflexive polytopes and thereby to mirror pairs of Calabi–Yau fourfolds. These lead to 532 600 483 distinct sets of Hodge numbers.

---

<sup>\*</sup>e-mail: schoeller@hep.itp.tuwien.ac.at

<sup>†</sup>e-mail: skarke@hep.itp.tuwien.ac.at

# 1 Introduction

When the relevance of Calabi–Yau manifolds to string compactification was first recognized [1], only very few such manifolds were known and it was hoped that a direct enumeration of all possibilities might lead to the identification of the string vacuum describing our universe. This hope has not been fulfilled. On the one hand there is still no general algorithm for a complete classification of all possible topologies of Calabi–Yau manifolds, and on the other hand it is by now understood that there are so many different constructions involving bundles, fluxes, D-branes etc. that probably even a complete list of all geometries would not get us very far.

Nevertheless it is important to have large lists of Calabi–Yau manifolds, both to scan for the possibility of finding standard model like physics, and to have a playground for doing statistics and checking hypotheses. Typically such lists are the results of solving classification problems for specific types of Calabi–Yau manifolds. The first computer aided classification was that of complete intersection Calabi–Yau threefolds [2], which resulted in 250 distinct pairs of Hodge numbers  $(h^{1,1}, h^{1,2})$ . A significantly larger list consists of hypersurfaces in weighted projective spaces, subject to the condition that the hypersurfaces feature no singularities beyond the ones already present in the ambient spaces. There are 7555 models of this type [3, 4], and together with 3284 similar models of Landau–Ginzburg type they lead to 2997 Hodge number pairs; including all abelian orbifolds of these models gives rise to 800 further pairs [5].

The richest source of models up to now has been toric geometry, a branch of algebraic geometry that allows for reasonably simple and explicit characterizations of algebraic varieties of dimension  $d$  in terms of elementary data pertaining to lattices of the type  $\mathbb{Z}^d$ . Calabi–Yau hypersurfaces in toric varieties can be described via reflexive polytopes [6]. A generalization via reflexive Gorenstein cones [7] provides data for gauged linear sigma models [8] that may correspond to higher codimension submanifolds in toric varieties, Landau–Ginzburg models or hybrids.

Reflexive polytopes of dimension  $d = 4$  account for the largest known list of Calabi–Yau threefolds. Their classification proceeded in two steps. First a set  $S$  of “maximal” polytopes was constructed, with the property that any reflexive polytope would have to be a subpolytope of one of the elements of  $S$ . Then the remaining (straightforward in principle but very tedious in practice) task was to find all subpolytopes of the elements of  $S$ . Any such maximal polytope can be described with the help of one or more weight systems (collections of positive numbers). The weight systems pertaining to reflexive 4–polytopes were found in Ref. [9]. There it was also shown that each of them gives rise to a maximal polytope that is actually reflexive, which is a property

$d$	$n_{\text{RP}}$	$\text{ld}(4 + \text{ld}(n_{\text{RP}})) - 1$
1	1	1
2	16	2
3	4319	3.0069
4	473 800 776	4.0365

Table 1: Numbers  $n_{\text{RP}}$  of reflexive polytopes of dimension  $d$  and a particular function of  $n_{\text{RP}}$  that involves two dual logarithms.

that need not hold for  $d > 4$ . Alternatively one can think of the weight system as defining a weighted projective space that can be partially resolved into a toric variety that contains a smooth Calabi–Yau hypersurface. This first step alone resulted already in 184 026 models and 10 237 sets of Hodge data. After an intermediate step of combining lower-dimensional weight systems into 17 320 further maximal polytopes [10] and several processor years of searching for subpolytopes, a list of 473 800 776 reflexive polytopes emerged [11]; these gave rise to 30 108 Hodge number pairs.

It should be possible to find many further Calabi–Yau threefolds by constructing reflexive Gorenstein cones. For this problem only the first step of classifying the pertinent weight systems has been taken [12].

With the advent of F–theory [13] Calabi–Yau fourfolds (at least elliptically fibred ones) acquired phenomenological relevance. The strategies for constructing threefolds can be applied to the fourfold case as well. Soon there existed the complete list of 1 100 055 hypersurfaces in weighted projective spaces [14] which gave rise to 667 954 triples of numbers  $(h^{1,1}, h^{1,2}, h^{1,3})$  (the only other nontrivial Hodge number  $h^{2,2}$  can be computed from these). More recently the (smaller) list of complete intersection fourfolds was also found [15].

Clearly we would expect much larger numbers of fourfolds from reflexive polytopes. An amusing way of obtaining a rough guess of the order of magnitude is by taking a look at Table 1. This table gives the number  $n_{\text{RP}}(d)$  of reflexive polytopes for every dimension  $d$  for which it is known, as well as the function

$$f(n_{\text{RP}}) = \text{ld}(4 + \text{ld}(n_{\text{RP}})) - 1 \quad (1)$$

of  $n_{\text{RP}}(d)$  which involves twice taking a logarithm with respect to base 2. As Table 1 shows,  $f(n_{\text{RP}}(d)) \geq d$ , with equality for  $d = 1, 2$  and small deviations for  $d = 3, 4$ . Upon inverting this to  $n_{\text{RP}}(d) \geq 2^{2^{d+1}-4}$  and assuming a similar relationship for  $d = 5$ , we would estimate  $n_{\text{RP}}(5)$  to exceed  $2^{2^6-4} \approx 1.15 \times 10^{18}$ . Since we lack the capacity to store more than a million TRPs (tera-reflexive-polytopes) we decided to aim for a more moderate goal.

The natural thing to do is, of course, to look for the weight systems

corresponding to  $d = 5$ . In the present paper we describe how we did that and what results we obtained. Section 2 contains a brief summary of the required concepts as well as an outline of the classification algorithm for reflexive polytopes. Section 3 describes our algorithm for finding the weight systems, which is an improved version of the one used in Refs. [9, 12]. Section 4 provides an illustration of the algorithm and section 5 is concerned with its implementation. In section 6 we present and discuss our results. An appendix contains a number of plots and diagrams that should make some of the rich structure of our data visible.

## 2 From Calabi–Yau manifolds to weights

### 2.1 General aspects

Toric geometry is usually formulated with reference to a dual pair of lattices  $M \simeq \mathbb{Z}^d$ ,  $N = \text{Hom}(M, \mathbb{Z})$  and their real extensions  $M_{\mathbb{R}} \simeq \mathbb{R}^d$ ,  $N_{\mathbb{R}} \simeq \mathbb{R}^d$ . A *lattice polytope*  $\Delta \subset M_{\mathbb{R}}$  is a polytope, i.e. the convex hull of a finite number of points, with vertices in  $M$ . We use the words polytope and polyhedron interchangeably. Following [16] we say that a polytope has the *IP property* (or, is an “IP polytope”) if the origin is in its interior. The *dual* of a set  $\Delta \subset M_{\mathbb{R}}$  is

$$\Delta^* = \{y \in N_{\mathbb{R}} : \langle y, x \rangle + 1 \geq 0 \quad \forall x \in \Delta\}; \quad (2)$$

the dual of an IP polytope  $\Delta$  is itself an IP polytope with  $\Delta^{**} = \Delta$ . An IP polytope  $\Delta$  is called *reflexive* if both  $\Delta$  and  $\Delta^*$  are lattice polytopes.

Batyrev [6] realized that mirror pairs of Calabi–Yau manifolds can be described via reflexive polytopes. The fan (i.e., set of cones) over some triangulation of the surface of  $\Delta^* \subset N_{\mathbb{R}}$  provides the data for a toric variety, and the lattice points of  $\Delta \subset M_{\mathbb{R}}$  correspond to the monomials occurring in the polynomial describing a Calabi–Yau hypersurface in that variety. In this context mirror symmetry just corresponds to swapping  $\Delta$  and  $\Delta^*$ . This symmetry manifests itself, in particular, by an exchange  $h^{i,j} \leftrightarrow h^{i,d-1-j}$  of the Hodge numbers of the corresponding  $(d-1)$ -dimensional Calabi–Yau manifolds. The following formula summarizes results of Batyrev [6] and Batyrev and Dais [17] for Hodge numbers of the type  $h^{1,i}$ :

$$\begin{aligned} h^{1,i} = & \delta_{1i} \left( l(\Delta^*) - d - 1 - \sum_{\text{codim } \theta^*=1} l_{\text{int}}(\theta^*) \right) \\ & + \delta_{d-2,i} \left( l(\Delta) - d - 1 - \sum_{\text{codim } \theta=1} l_{\text{int}}(\theta) \right) \\ & + \sum_{\text{codim } \theta^*=i+1} l_{\text{int}}(\theta^*) l_{\text{int}}(\theta). \end{aligned} \quad (3)$$

Here  $l$  gives the number of lattice points of some polytope and  $l_{\text{int}}$  the number of interior lattice points;  $\theta$  and  $\theta^*$  denote mutually dual faces of  $\Delta$  and  $\Delta^*$ , respectively, with codimensions as indicated under the summation symbols. For the present case of Calabi–Yau fourfolds (i.e.  $d = 5$ ) the only further non-trivial Hodge number is  $h^{2,2}$  which depends on the others via the well known relation

$$h^{2,2} = 44 + 4h^{1,1} - 2h^{1,2} + 4h^{1,3}. \quad (4)$$

## 2.2 Classification of reflexive polytopes

The main idea of the classification algorithm of [18, 19] is to look for a set  $S = \{\Delta_1, \Delta_2, \dots\}$  of lattice polytopes such that any reflexive polytope  $\Delta$  is contained in at least one of the  $\Delta_i$ . Since duality inverts subset relations,  $\Delta \subseteq \tilde{\Delta} \iff \Delta^* \supseteq \tilde{\Delta}^*$ , every reflexive polytope must then contain at least one of  $\Delta_1^*, \Delta_2^*, \dots$ .

This motivates the definition of a *minimal polytope*  $\nabla \subset N_{\mathbb{R}}$  as a polytope that has the IP property, whereas the convex hull of any proper subset of the set of its vertices fails to have it.

Properties of minimal polytopes were analysed in [18]. It turns out that a minimal polytope is either a simplex with the origin in the interior (“IP simplex”) or the convex hull of a number of lower-dimensional simplices of that type; for any given dimension there is a finite number of combinatorial ways in which a minimal polytope can consist of several lower-dimensional IP simplices. To any IP simplex of dimension  $d$  with vertices  $V_1, \dots, V_{d+1}$  we can assign a *weight system* (array of weights)  $\mathbf{q} \in \mathbb{R}_{>0}^{d+1}$  via  $\sum_i q_i V_i = 0$ . The definition of  $\mathbf{q}$  is unique up to rescaling. In the case where the  $V_i$  are lattice points we can use this freedom to make the  $q_i$  integer; alternatively we can use a convention such as  $\sum_i q_i = 1$ . Minimal polytopes consisting of more than one IP simplex are described by *combined weight systems* (matrices of weights).

Given a minimal polytope  $\nabla$  constructed with a (combined) weight system, its dual  $\nabla^*$  will usually not be a lattice polytope. In order to be relevant for our classification problem,  $\nabla^*$  must however contain a lattice polytope with the IP property. This statement only makes sense once we know to which pair of lattices we are referring. The coarsest lattice for which  $\nabla$  is a lattice polytope is just the lattice linearly generated by the vertices of  $\nabla$ ; this lattice  $N_{\text{coarsest}}$ , which is determined by the (combined) weight system, must be a sublattice of any other lattice  $N$  that contains the vertices of  $\nabla$ . Then  $N_{\text{coarsest}} \subseteq N$  implies  $M \subseteq M_{\text{finest}}$  (the lattice dual to  $N_{\text{coarsest}}$ ), so the convex hull  $\text{conv}(\nabla^* \cap M)$  can have the IP property only if  $\text{conv}(\nabla^* \cap M_{\text{finest}})$  has it.

We say that a (combined) weight system has the IP property if  $\text{conv}(\nabla^* \cap M_{\text{finest}})$  has it, where  $\nabla$  is the corresponding minimal polytope. One can

easily show [19] that, for a combined weight system to have the IP property, it is necessary that every single weight system occurring in it has this property; we shall refer to such weight systems as IP weight systems.

In Ref. [9] the IP weight systems for  $d \leq 4$  were found: there are 3/95/184 026 for  $d$  equal to 2/3/4, respectively. In addition there are 1/21/17 320 combined weight systems giving rise to non-simplicial 2/3/4-dimensional minimal polytopes with the IP property [10]. The remaining task in the classification [11, 16] of all reflexive polytopes of dimension up to 4 was to find all reflexive subpolytopes (both on  $M_{\text{finest}}$  and on its sublattices) of these 4/116/201 346 polytopes and to ensure that every isomorphism class of polytopes was counted only once; this was achieved by the introduction of a suitable normal form for reflexive polytopes.

In the present work we report how we found all weight systems with the IP property for  $d = 5$ .

### 3 Algorithm

Given a weight system  $\mathbf{q}$  we need an efficient description of the polytope determined by  $\mathbf{q}$ . This is achieved as follows [18, 19]. If  $V_1, \dots, V_n$  are the vertices of  $\nabla$  satisfying  $\sum_i q_i V_i = 0$ , we define an embedding map for  $\nabla^* \subset M_{\mathbb{R}}$  via

$$M_{\mathbb{R}} \rightarrow \mathbb{R}^n, \quad X \mapsto \mathbf{y} = (y_1, \dots, y_n) \text{ with } y_i = \langle V_i, X \rangle. \quad (5)$$

Under this map the image of  $M_{\mathbb{R}}$  is the linear subspace of  $\mathbb{R}^n$  for which  $\sum_i q_i y_i = 0$ . The image of  $\nabla^*$  also satisfies  $y_i \geq -1$  for all  $i$ , and the image of  $M_{\text{finest}}$  is  $\mathbb{Z}^n \cap \{\mathbf{y} : \sum_i q_i y_i = 0\}$ . Here we have  $n = d + 1$ , but the same construction works for a combination of  $k$  weight systems and  $n = d + k$ .

Clearly  $\mathbf{q}$  has the IP property if and only if  $\mathbf{0}$  is in the interior of the convex hull of

$$\mathbb{Z}^n \cap \{\mathbf{y} : \sum_i q_i y_i = 0, y_i \geq -1 \forall i\}. \quad (6)$$

Upon passing to new coordinates  $x_i = y_i + 1$  (and thereby turning our linear subspace into an affine one) the condition  $\sum_i q_i y_i = 0$  changes to  $\sum_i x_i q_i = r$  whereby the normalization  $r = \sum_i q_i$  becomes relevant. For  $r = 1$  we can restate the IP condition as  $(1, \dots, 1) \in \text{int}(\Delta_{\mathbf{q}})$  with

$$\Delta_{\mathbf{q}} = \text{conv}(\{(x_1, \dots, x_n) : x_i \in \mathbb{Z}_{\geq 0}, \sum_i x_i q_i = 1\}). \quad (7)$$

This can hold only if all weights obey  $q_i \leq 1/2$  (if  $q_i > 1/2$  then  $x_i \in \{0, 1\}$  for all  $\mathbf{x} \in \Delta_{\mathbf{q}}$ , leading to a violation of the IP condition). For  $n > 2$  at most one of the  $q_i$  can be equal to  $1/2$  (otherwise  $\sum_i q_i > 1$ ). Furthermore it is not difficult to see that for  $q_n = 1/2$  the IP condition amounts to

$(2, \dots, 2) \in \text{int}(\Delta_{(q_1, \dots, q_{n-1})})$ . This allows us to restrict our attention to weights smaller than  $1/2$ , with a convenient split of our problem into finding  $n = 6$  weights with  $r = 1$  and  $(1, 1, 1, 1, 1, 1) \in \text{int}(\Delta_{\mathbf{q}})$  or  $n = 5$  weights with  $r = 1/2$  and  $(2, 2, 2, 2, 2) \in \text{int}(\Delta_{\mathbf{q}})$ , respectively.

Any set of  $n$  linearly independent  $\mathbf{x}^{(i)} \in \Delta_{\mathbf{q}}$  will determine  $\mathbf{q}$ . We use this fact for the classification, starting with  $\mathbf{x}^{(0)} = (1, \dots, 1)$  or  $(2, \dots, 2)$  and continuing by successively adding further lattice points  $\mathbf{x}^{(i)}$ , thereby restricting the set of allowed  $\mathbf{q}$ 's. Having chosen  $\mathbf{x}^{(0)}, \dots, \mathbf{x}^{(k)}$  we can pick an arbitrary  $\tilde{\mathbf{q}}$  such that  $\mathbf{x}^{(j)} \cdot \tilde{\mathbf{q}} = 1$  (with  $\mathbf{x} \cdot \mathbf{q} := \sum_i x_i q_i$ ) for all  $j = 0, \dots, k$ ; if  $\tilde{\mathbf{q}}$  has the IP property we add it to our list. If  $k + 1 = n$  then  $\tilde{\mathbf{q}}$  is the unique weight system compatible with  $\mathbf{x}^{(0)}, \dots, \mathbf{x}^{(k)}$  and we are finished with this branch of the construction. Otherwise, note that  $\mathbf{x}^{(0)}$  (which satisfies  $\mathbf{x}^{(0)} \cdot \tilde{\mathbf{q}} = 1$ ) cannot be interior to  $\Delta_{\mathbf{q}}$  for  $\mathbf{q} \neq \tilde{\mathbf{q}}$  unless  $\Delta_{\mathbf{q}}$  contains points satisfying  $\mathbf{x} \cdot \tilde{\mathbf{q}} < 1$ . Therefore it suffices to consider each of the finitely many lattice points obeying  $x_i \geq 0$  for all  $i$  and  $\mathbf{x} \cdot \tilde{\mathbf{q}} < 1$  as the next chosen point  $\mathbf{x}^{(k+1)}$ . Given the finite number of choices at each branching level  $k \in \{0, \dots, n - 2\}$  we are bound to eventually find all allowed weight systems.

As in [12] we use the following method for finding suitable  $\tilde{\mathbf{q}}$ 's. Every set of linearly independent  $\mathbf{x}^{(0)}, \dots, \mathbf{x}^{(k)}$  determines the  $(n - k - 1)$ -dimensional polytope

$$\{\mathbf{q} : q_i \geq 0, \mathbf{x}^{(j)} \cdot \mathbf{q} = 1 \forall j = 0, \dots, k\} \quad (8)$$

in  $\mathbf{q}$ -space. The vertices of this polytope can be computed efficiently by using the  $(n - k)$ -dimensional polytope of the previous step. We simply take  $\tilde{\mathbf{q}}^{(k)}$  as the average of these vertices.

The algorithm as presented so far has the disadvantage of finding weight systems many times, both in terms of identical copies  $\mathbf{q}' = \mathbf{q}$  and of permutation equivalent ones,  $q'_i = q_{\pi(i)}$ , where  $\pi$  represents an element of the group  $S_n$  of permutations of the coordinates.

The following strategy gets rid of identical copies almost completely. Essentially, if we want to find a given weight system  $\mathbf{q}$  precisely once, there must be a unique sequence of  $\mathbf{x}^{(i)}$  resulting in  $\mathbf{q}$ . Such a sequence can be defined by  $\mathbf{x}^{(k+1)}$  being the lattice point in  $\Delta_{\mathbf{q}}$  that minimizes  $\mathbf{x} \cdot \tilde{\mathbf{q}}^{(k)}$ ; if the minimum value occurs for more than one lattice point,  $\mathbf{x}^{(k+1)}$  is taken as the lexicographically largest one among them (this is equivalent to a very small deformation of  $\tilde{\mathbf{q}}^{(k)}$ ). This results in a unique sequence of lattice points  $\mathbf{x}^{(0)}, \mathbf{x}^{(1)}, \dots, \mathbf{x}^{(n-1)}$  defining  $\mathbf{q}$  except in those rare cases in which  $\mathbf{q} = \tilde{\mathbf{q}}^{(k)}$  for some  $k < n - 1$ . During the execution of the algorithm  $\mathbf{q}$  is of course not yet known. The conditions defined above are implemented as follows: given  $\mathbf{x}^{(0)}, \dots, \mathbf{x}^{(k)}$  we determine the set of all nonnegative lattice points in the affine space spanned by them and abandon this branch of the recursion unless all of  $\mathbf{x}^{(0)}, \dots, \mathbf{x}^{(k)}$  satisfy the above criteria within that space.

Redundancies from permutation equivalences can be reduced by keeping

track of which subgroup  $G^{(k)}$  of the original group  $G^{(0)} = S_n$  of coordinate permutations leaves each of the points  $\mathbf{x}^{(0)}, \dots, \mathbf{x}^{(k)}$  invariant; then one proceeds with a given  $\mathbf{x}^{(k+1)}$  only if it is the lexicographically largest one within its  $G^{(k)}$ -orbit.

Very explicitly, having computed  $\tilde{\mathbf{q}}^{(k-1)}$  our algorithm determines all points  $\mathbf{x}^{(k)} \in \mathbb{Z}_{\geq 0}^n$  with  $\mathbf{x}^{(k)} \cdot \tilde{\mathbf{q}}^{(k-1)} < 1$  and rejects the new point  $\mathbf{x}^{(k)}$  if any of the following conditions, which are checked in the given order, holds:

1.  $x_i^{(k)} \leq 1/r$  for all  $i$ ,
2.  $\sum_i x_i^{(k)} \leq 2$ ,
3.  $\mathbf{x}^{(k)}$  is not the lexicographically largest after application of allowed coordinate permutations,
4. (a)  $\mathbf{x}^{(k)} \cdot \tilde{\mathbf{q}}^{(j)} < \mathbf{x}^{(j+1)} \cdot \tilde{\mathbf{q}}^{(j)}$  or  
 (b)  $\mathbf{x}^{(k)} \cdot \tilde{\mathbf{q}}^{(j)} = \mathbf{x}^{(j+1)} \cdot \tilde{\mathbf{q}}^{(j)}$  and  $\mathbf{x}^{(k)} > \mathbf{x}^{(j+1)}$   
 for some  $j < k - 1$ ,
5. for some  $j < k$  there exists a point  $\mathbf{x}$  with  $x_i \geq 0$  that lies on the line through  $\mathbf{x}^{(k)}$  and  $\mathbf{x}^{(j)}$  but not between  $\mathbf{x}^{(k)}$  and  $\mathbf{x}^{(j)}$ ,
6. the sequence  $\mathbf{x}^{(0)}, \dots, \mathbf{x}^{(k)}$  does not allow a positive weight system,
7. the set of nonnegative lattice points in the affine span of  $\{\mathbf{x}^{(0)}, \dots, \mathbf{x}^{(k)}\}$  (which is computed as the set of  $\mathbf{x} \in \Delta_{\tilde{\mathbf{q}}^{(k)}}$  that have an inner product of 1 with every vertex of the  $\mathbf{q}$ -space polytope (8)) contains an  $\mathbf{x}$  with  
 (a)  $\mathbf{x} \cdot \tilde{\mathbf{q}}^{(j)} < \mathbf{x}^{(j+1)} \cdot \tilde{\mathbf{q}}^{(j)}$  or  
 (b)  $\mathbf{x} \cdot \tilde{\mathbf{q}}^{(j)} = \mathbf{x}^{(j+1)} \cdot \tilde{\mathbf{q}}^{(j)}$  and  $\mathbf{x} > \mathbf{x}^{(j+1)}$   
 for some  $j < k$ .

These checks are not independent: items 1 and 2 each imply number 6 and items 4 and 5 each imply number 7. The earlier checks are included because they are so much simpler than the later ones that they result in a reduction of computation time.

## 4 Illustration of the algorithm

In this section we will demonstrate explicitly how our algorithm works by following a specific path in the recursive tree for  $n = 5$ ,  $r = 1/2$  from the root at  $\mathbf{x}^{(0)} = (2, 2, 2, 2, 2)$  to its tip. We will explain at each branch point some of



the considerations that play a role, with references to specific items in the list at the end of the last section.

We start with the subset of  $\mathbf{q}$ -space defined by  $q_i \geq 0$ . The condition  $\sum_i q_i = r = 1/2$ , which is equivalent to  $\mathbf{x}^{(0)} \cdot \mathbf{q} = 1$ , determines a simplex in  $\mathbf{q}$ -space which we describe by the matrix

$$\begin{pmatrix} 1/2 & 0 & 0 & 0 & 0 \\ 0 & 1/2 & 0 & 0 & 0 \\ 0 & 0 & 1/2 & 0 & 0 \\ 0 & 0 & 0 & 1/2 & 0 \\ 0 & 0 & 0 & 0 & 1/2 \end{pmatrix}; \quad (9)$$

here and later we encode a  $\mathbf{q}$ -space polytope by a matrix whose lines correspond to the vertices. The average of the vertices gives the first candidate for an IP weight system:

$$\tilde{\mathbf{q}}^{(0)} = (1/10, 1/10, 1/10, 1/10, 1/10). \quad (10)$$

**Point 1**

The point  $\mathbf{x}^{(1)}$  must satisfy  $x_i^{(1)} \in \mathbb{Z}_{\geq 0}$  and  $\mathbf{x}^{(1)} \cdot \tilde{\mathbf{q}}^{(0)} < 1$ , i.e.,  $\sum_i x_i^{(1)} < 10$ . Points  $\mathbf{x}$  with  $x_i \leq 1/r = 2$  for all  $i$  do not lead to positive weight systems so they are excluded (cf. item 1). There are 1760 points that satisfy the conditions. Taking only the lexicographically largest ones from orbits of coordinate permutations (cf. item 3) reduces the number to 63 points:  $(9, 0, 0, 0, 0)$ ,  $(8, 1, 0, 0, 0)$ ,  $(8, 0, 0, 0, 0)$ ,  $(7, 2, 0, 0, 0)$ ,  $(7, 1, 1, 0, 0)$ ,  $\dots$ ,  $(3, 0, 0, 0, 0)$ . Furthermore, the points  $(3, 1, 1, 1, 1)$ ,  $(3, 2, 1, 1, 1)$ ,  $(3, 2, 2, 1, 1)$ ,  $(3, 3, 1, 1, 1)$ ,  $(4, 1, 1, 1, 1)$ ,  $(4, 2, 1, 1, 1)$ , and  $(5, 1, 1, 1, 1)$  all are excluded because they lie on lines between  $(2, 2, 2, 2, 2)$  and another allowed point (cf. item 5), thereby violating minimality of  $\mathbf{x}^{(1)} \cdot \tilde{\mathbf{q}}^{(0)}$ . This leads to 56 allowed points. For this example we pick the point

$$\mathbf{x}^{(1)} = (3, 0, 0, 0, 0). \quad (11)$$

The condition  $\mathbf{x}^{(1)} \cdot \mathbf{q} = 1$  restricts the allowed region in  $\mathbf{q}$ -space to the simplex

$$\begin{pmatrix} 1/3 & 1/6 & 0 & 0 & 0 \\ 1/3 & 0 & 1/6 & 0 & 0 \\ 1/3 & 0 & 0 & 1/6 & 0 \\ 1/3 & 0 & 0 & 0 & 1/6 \end{pmatrix}, \quad (12)$$

and we find another candidate for an IP weight system:

$$\tilde{\mathbf{q}}^{(1)} = (1/3, 1/24, 1/24, 1/24, 1/24). \quad (13)$$

**Point 2**

At this stage, up to coordinate permutations, there are 1164 choices for the point  $\mathbf{x}^{(2)}$  that lead to positive weight systems. Some of those are excluded by demanding that  $\mathbf{x}^{(k+1)} \cdot \tilde{\mathbf{q}}^{(k)}$  is minimal among all points leading to the same final  $\mathbf{q}^{(4)}$  (cf. item 7). For example, the choice  $\mathbf{x}^{(2)} = (0, 7, 3, 3, 3)$  is not allowed because  $\mathbf{x} \cdot \tilde{\mathbf{q}}^{(1)} < \mathbf{x}^{(2)} \cdot \tilde{\mathbf{q}}^{(1)}$  for  $\mathbf{x} = \mathbf{x}^{(0)} + 2(\mathbf{x}^{(1)} - \mathbf{x}^{(0)}) + 2(\mathbf{x}^{(2)} - \mathbf{x}^{(0)}) = (0, 8, 0, 0, 0)$ . This leaves us with 803 candidates, one of them being

$$\mathbf{x}^{(2)} = (0, 7, 4, 0, 0). \quad (14)$$

This point leads to the polytope

$$\begin{pmatrix} 1/3 & 1/9 & 1/18 & 0 & 0 \\ 1/3 & 1/7 & 0 & 1/42 & 0 \\ 1/3 & 1/7 & 0 & 0 & 1/42 \end{pmatrix} \quad (15)$$

in  $\mathbf{q}$ -space and the weight system

$$\tilde{\mathbf{q}}^{(2)} = (1/3, 25/189, 1/54, 1/126, 1/126). \quad (16)$$

**Point 3**

Again there is a large number of nonnegative points satisfying  $\mathbf{x} \cdot \tilde{\mathbf{q}}^{(2)} < 1$ . As an illustration of our rule that lexicographic ordering serves as a tie-breaker if more than one  $\mathbf{x}$  minimizes  $\mathbf{x} \cdot \tilde{\mathbf{q}}^{(k)}$  (item 7b) consider the possible choice of  $\mathbf{x}^{(3)} = (1, 0, 0, 3, 0)$ . This is not permitted because  $\mathbf{x}^{(3)} \cdot \tilde{\mathbf{q}}^{(1)} = \mathbf{x}^{(2)} \cdot \tilde{\mathbf{q}}^{(1)}$  and  $\mathbf{x}^{(3)} > \mathbf{x}^{(2)}$ , thereby violating the requirement that  $\mathbf{x}^{(2)}$  is the lexicographically largest point that minimizes  $\mathbf{x} \cdot \tilde{\mathbf{q}}^{(1)}$ . An allowed choice is

$$\mathbf{x}^{(3)} = (0, 0, 0, 43, 0), \quad (17)$$

so that the polytope in  $\mathbf{q}$ -space becomes

$$\begin{pmatrix} 1/3 & 55/387 & 1/774 & 1/43 & 0 \\ 1/3 & 1/7 & 0 & 1/43 & 1/1806 \end{pmatrix}. \quad (18)$$

As explained in section 5, this is one of the pairs of 5-tuples that are gathered and processed later for performance reasons. For this example we just continue the algorithm and find the weight system

$$\tilde{\mathbf{q}}^{(3)} = (1/3, 386/2709, 1/1548, 1/43, 1/3612). \quad (19)$$

**Point 4**

For the final step we choose the point

$$\mathbf{x}^{(4)} = (0, 7, 0, 0, 1), \quad (20)$$

weight system	$h^{1,1}$	$h^{1,2}$	$h^{1,3}$	$n_p$	$n_v$	$n_f$
$\hat{\mathbf{q}}^{(0)}$	1	0	976	1128	6	6
$\hat{\mathbf{q}}^{(1)}$	2	0	3878	4551	6	6
$\hat{\mathbf{q}}^{(2)}$	43	3	4884	5709	10	8
$\hat{\mathbf{q}}^{(3)}$	912	0	43544	51069	9	9
$\hat{\mathbf{q}}^{(4)}$	not reflexive			197084	10	8

Table 2: Hodge numbers, number of points  $n_p$ , number of vertices  $n_v$ , and number of faces  $n_f$  of the polytopes corresponding to the weight systems (22) obtained in the example.

leading to the weight system

$$\tilde{\mathbf{q}}^{(4)} = (1/3, 571/3999, 1/7998, 1/43, 2/3999). \quad (21)$$

We have now collected five  $n = 5$ ,  $r = 1/2$  weight systems. To be relevant for our classification of polytopes in five dimensions, we have to add a weight of one half, such that we obtain weight systems with  $n = 6$ ,  $r = 1$ :

$$\begin{aligned} \hat{\mathbf{q}}^{(0)} &= (1/2, 1/10, 1/10, 1/10, 1/10, 1/10), \\ \hat{\mathbf{q}}^{(1)} &= (1/2, 1/3, 1/24, 1/24, 1/24, 1/24), \\ \hat{\mathbf{q}}^{(2)} &= (1/2, 1/3, 25/189, 1/54, 1/126, 1/126), \\ \hat{\mathbf{q}}^{(3)} &= (1/2, 1/3, 386/2709, 1/1548, 1/43, 1/3612), \\ \hat{\mathbf{q}}^{(4)} &= (1/2, 1/3, 571/3999, 1/7998, 1/43, 2/3999). \end{aligned} \quad (22)$$

Finally, the IP check and calculation of Hodge numbers and point numbers can be performed with the result found in Table 2.

As a side remark we mention that, while it is fairly typical that the  $\mathbf{q}$ -space polytopes are simplices (as they were in the present example), this is of course not necessary.

## 5 Implementation

Our starting point was the implementation of the algorithm in PALP 2.1 [20, 21] as it was used for constructing weight systems for reflexive Gorenstein cones [12]. While the actual classification algorithm was rewritten in C++, the check for the IP property and reflexivity was delegated to PALP's existing highly optimized C routines. For the Hodge number computation we relied, as described below, on an improved version of PALP's C code. The programs were compiled with *UndefinedBehaviorSanitizer* enabled using the flags `-fsanitize=signed-integer-overflow` and `-fsanitize=undefined-`

**trap-on-error.** This ensures that signed integer arithmetic overflows are detected during run time.

After we improved redundancy avoidance along the lines indicated in the last paragraphs of section 3, some experimentation showed that it was most efficient to apply it only at the upper levels of the recursion tree since it tended to be quite time consuming if used at every node. With redundancy avoidance turned off at the two lowest branching levels, it was possible to run the algorithm on a single machine down to the last branching level within 7 minutes for the case  $n = 6, r = 1$  and within 4 minutes for the case  $n = 5, r = 1/2$ . At that level the allowed polytope (8) in  $\mathbf{q}$ -space is one-dimensional, i.e. it is a line segment bounded by two  $n$ -tuples with nonnegative entries as illustrated in (18). These data were sorted and residual redundancies were removed, resulting in 46 739 902 pairs of 5-tuples and 59 048 418 pairs of 6-tuples which were then distributed to 6 PCs for the last level of the recursion. After roughly 53 hours on each machine, a total of 640 core hours, we obtained approximately  $5.1 \times 10^{11}$  weight systems which amounted to 5.3 TB of data. The weight systems were sorted and after duplicates were removed the result consisted of 108 340 852 387 candidates for  $n = 6, r = 1$  and 228 960 353 952 candidates for  $n = 5, r = 1/2$ .

These weight systems still needed to be checked for the IP property and reflexivity; in the reflexive case we would also want to compute the corresponding Hodge numbers. While PALP's IP-check was made very efficient for the classification of reflexive polytopes in 4d, the Hodge number computation had not been a bottleneck so far. In the present project, however, this was different.

In order to construct a pair of polytopes as well as the corresponding set of Hodge numbers from a weight system  $\mathbf{q}$ , the following steps have to be taken. The lattice points (6) must be enumerated and the equations describing the facets of the polytope that forms their convex hull (i.e. the polytope  $\Delta_{\mathbf{q}}$  of eq. (7), up to the coordinate shift which we ignore here) must be computed. PALP is good at these tasks and there was no need for improvement. If  $\Delta_{\mathbf{q}}$  is reflexive then all of its equations will correspond to integer points in the dual lattice, thereby providing the vertices of  $\Delta_{\mathbf{q}}^*$ . In order to evaluate formula (3) for the Hodge numbers  $h^{1,i}$  we also require information on the faces of  $\Delta_{\mathbf{q}}$  and  $\Delta_{\mathbf{q}}^*$  and on the numbers  $l(\theta)$  of lattice points and  $l_{\text{int}}(\theta)$  of interior lattice points on a face  $\theta$ . PALP has efficient routines for analysing the face structure by using bit patterns [20,21], which also perform well in the present context. Finally, the point counting works as follows. PALP creates a complete list of lattice points of  $\Delta_{\mathbf{q}}^*$  by first identifying a parallelepiped  $P$  that contains all the vertices of  $\Delta_{\mathbf{q}}^*$  ( $P$  is bounded by  $n$  of the hyperplanes bounding  $\Delta_{\mathbf{q}}$  as well as hyperplanes parallel to these), checking for every lattice point of  $P$  whether it belongs to  $\Delta_{\mathbf{q}}^*$ , and adding such a point to the

list if it does; examining all lattice points of  $P$  corresponds to a nested set of loops in the program. Then PALP goes over the complete list of points and the complete list of faces and raises  $l_{\text{int}}$  of the face if appropriate. Here we achieved a considerable upgrade of efficiency. We improved the conditions upon which the program exits from a particular loop. Furthermore, instead of creating the full set of lattice points of  $\Delta_{\mathbf{q}}^*$  we used the following trick. The innermost loop level corresponds to a sequence of lattice points along a line in  $\Delta_{\mathbf{q}}^*$ . Having worked out to which faces the first and last point in the line are interior, all other points must be interior to the affine span of these faces, and we can immediately raise the corresponding numbers  $l_{\text{int}}$  with the appropriate multiplicities, without having to create and analyse the full list.

Despite these improvements it would have taken a long time to process all candidate weight systems on our local computers. We therefore used the facilities of the Vienna Scientific Cluster (VSC-3). The IP check and Hodge number calculation for the 337 301 206 339 weight system candidates was distributed among 119 nodes and completed in 57 321 core hours on machines with Intel Xeon E5-2650 v2 processors clocked at 2.6 GHz.

Weight systems that determine reflexive polytopes were sorted according to their Hodge numbers, the ones leading to non-reflexive polytopes according to vertex count, facet count, and point count. All of them were stored in a PostgreSQL database.

Then we compared our results with the two largest existing lists of weight systems. One of them is the complete list of IP weight systems with  $\sum_{i=1}^6 q_i \leq 300$  (in the normalization in which the  $q_i$  are integer) which was generated by considering suitable partitions of the numbers up to 300 (to be found at the website [22]; it represents a straightforward generalization of the list up to  $\sum_{i=1}^6 q_i \leq 150$  presented in [23]). The other one was the complete list of 1 100 055 hypersurfaces in weighted projective spaces [14]. We confirmed that every single weight system occurring in either of these lists could be found in the database. Since the construction of our database was completely independent both conceptually and computationally from the way these lists were generated, it seems very unlikely that there is an error in our algorithm or programming. Together with the fact that we excluded the possibility of numerical errors from overflows, which might have led to misinterpreting viable weight systems as non-IP, this gives us quite an amount of confidence in the reliability of our results.

## 6 Results and discussion

There are 322 383 760 930 weight systems with six weights that determine five-dimensional polytopes with the IP property. 185 269 499 015 of these polyhedra are reflexive, 137 114 261 915 non-reflexive. The PostgreSQL database

	$h^{1,1}$	$h^{1,2}$	$h^{1,3}$	$h^{2,2}$	$\chi$	weight system count
1	25 827	0	13	103 404	155 088	660 386 443
2	28 348	0	12	113 484	170 208	650 642 665
3	23 426	0	14	93 804	140 688	388 024 998
4	22 386	0	15	89 648	134 454	323 589 412
5	30 989	0	11	124 044	186 048	289 288 747
6	24 738	0	14	99 052	148 560	239 597 804
7	23 946	0	14	95 884	143 808	230 489 503
8	25 746	0	14	103 084	154 608	211 084 163
9	27 548	0	12	110 284	165 408	193 560 096
10	20 154	0	16	80 724	121 068	190 167 835

Table 3: The ten most frequent sets of Hodge numbers.

which contains all of these data is searchable via a web front-end at:

<http://rgc.itp.tuwien.ac.at/fourfolds>

The reflexive polytopes give rise to 532 600 483 distinct sets of Hodge numbers. Thus a Hodge number triple in our list occurs on average for roughly 350 weight systems. This number is, of course, just the mean of a strongly skewed distribution. The Hodge data sets with the highest numbers of occurrences are shown in Table 3.

One should note that distinct weight systems may well lead to the same polytope (we have not checked how often this occurs). In particular it seems that polytopes with a small number of lattice points are generated many times, which accounts for the fact that  $h^{1,1} \gg h^{1,3}$  for all the entries of Table 3. The Hodge numbers  $h^{i,j}$  and the Euler characteristic  $\chi$  of the reflexive polyhedra lie within the following ranges:

- $1 \leq h^{1,1} \leq 303\,148$  (with 190 201 distinct values),
- $0 \leq h^{1,2} \leq 2010$  (with 1689 distinct values),
- $1 \leq h^{1,3} \leq 303\,148$  (with 145 848 distinct values),
- $82 \leq h^{2,2} \leq 1\,213\,644$  (with 361 426 distinct values),
- $-252 \leq \chi \leq 1\,820\,448$  (with 188 804 distinct values).

The appendix to this paper contains a number of figures with which we try to visualize our data. Because of formula (4) and the standard dependence of  $\chi$  on the Hodge numbers, the space of quintuples  $(h^{1,1}, h^{1,2}, h^{1,3}, h^{2,2}, \chi)$  is really a three-dimensional data set. Due to the size of this set we found no

way of adequately visualizing it in its full dimensionality. Instead we have mainly relied on the two-dimensional plot of  $(h^{1,1}, h^{1,3})$ , i.e. numbers of Kähler and complex structure moduli, which is the straightforward generalization of the usual Hodge number plot for threefolds. It is also the most natural choice in the sense that the missing direction is the one along which our data set is thinnest (as one sees from the list above, the ranges for  $h^{1,1}$  and  $h^{1,3}$  are larger by a factor of  $\sim 150$  than that for  $h^{1,2}$ ).

Fig. 1 presents the shape of the whole dataset. Similarly to the corresponding set for threefolds, it is dense (in the sense that every possible pair occurs) in a large region with moderate values of  $h^{1,1}$  and  $h^{1,3}$  and shows a characteristic symmetric shape with three peaks and a grid structure related to fibrations whose fibres correspond to self-dual polyhedra of one dimension less [24]. Apparently the set of tips in any dimension can be described in the following manner. Consider the sequence of integers

$$(a_i) = (2, 3, 7, 43, 1807, \dots) \quad (23)$$

generated by the rule

$$a_1 = 2, \quad a_{n+1} = 1 + \prod_{i=1}^n a_i = a_n(a_n - 1) + 1. \quad (24)$$

It is easy to show by induction that

$$\sum_{i=1}^n \frac{1}{a_i} = 1 - \frac{1}{\prod_{i=1}^n a_i}, \quad (25)$$

which implies that the  $n$ -tuples

$$\mathbf{q}_{\text{ct}}^{(n)} = \left( \frac{1}{a_1}, \dots, \frac{1}{a_{n-1}}, \frac{1}{\prod_{i=1}^{n-1} a_i} \right), \quad (26)$$

$$\mathbf{q}_{\text{lt}}^{(n)} = \left( \frac{1}{a_1}, \dots, \frac{1}{a_{n-2}}, \frac{1}{2 \prod_{i=1}^{n-2} a_i}, \frac{1}{2 \prod_{i=1}^{n-2} a_i} \right) \quad (27)$$

form weight systems with  $\sum q_i = 1$ . Since each weight is the inverse of an integer (i.e. they are ‘‘Fermat weights’’) both of these weight systems have the IP property. Comparison with our data shows that

$$\mathbf{q}_{\text{ct}}^{(6)} = \left( \frac{1}{2}, \frac{1}{3}, \frac{1}{7}, \frac{1}{43}, \frac{1}{1807}, \frac{1}{3263442} \right) \quad \text{and} \quad \mathbf{q}_{\text{lt}}^{(6)} = \left( \frac{1}{2}, \frac{1}{3}, \frac{1}{7}, \frac{1}{43}, \frac{1}{3612}, \frac{1}{3612} \right)$$

correspond to the central upper tip and to the left tip in Fig. 1, respectively. The analogous statements for Calabi–Yau threefolds ( $n = 5$ ) are also easily

checked. The right upper tip corresponds of course to the polytope that is dual to the one determined by  $\mathbf{q}_{\text{lt}}$ . If we represent  $\Delta_{\mathbf{q}_{\text{lt}}^{(n)}}$  and  $\Delta_{\mathbf{q}_{\text{ct}}^{(n)}}$  as in (7), so that the interior lattice point is  $(1, \dots, 1)$ , it is easy to see that the intersection of either of these polytopes with the hyperplane  $x_{n-1} = x_n$  is isomorphic to  $\Delta_{\mathbf{q}_{\text{ct}}^{(n-1)}}$ ; likewise  $\Delta_{\mathbf{q}_{\text{lt}}^{(n)}}$ , which is isomorphic to  $\Delta_{\mathbf{q}_{\text{lt}}^{(n)}}$  up to a change of lattice, has  $\Delta_{\mathbf{q}_{\text{ct}}^{(n-1)}}$  as a subpolytope. These inclusions of reflexive polyhedra give rise to fibration structures where the fibre is the self-mirror Calabi–Yau manifold of dimension one less that corresponds to  $\Delta_{\mathbf{q}_{\text{ct}}^{(n-1)}}$ ; see Ref. [24] for details of this construction and how it can be used to explain the structure of the uppermost part of the Hodge number plot. A further fibration structure comes from the fact that  $\Delta_{\mathbf{q}_{\text{lt}}^{(n)}}$  has a subpolytope isomorphic to  $\Delta_{\mathbf{q}_{\text{lt}}^{(n-1)}}$  in the hyperplane  $2x_{n-2} = x_{n-1} + x_n$ . In the case of  $n = 4$  the two inclusions  $\Delta_{(1/2, 1/3, 1/12, 1/12)} \supset \Delta_{(1/2, 1/3, 1/6)}$  and  $\Delta_{(1/2, 1/3, 1/12, 1/12)} \supset \Delta_{(1/2, 1/4, 1/4)}$  correspond to distinct elliptic fibration structures of a K3 manifold that are related to  $E_8 \times E_8$  [25] and  $SO(32)$  [26], respectively; via further nested inclusions these elliptic fibration structures occur in higher dimensions as well.

Among Figs. 2 to 6, each corresponds to the small subregion of the previous plot that is indicated by the rectangle bounded by dashed lines. With the exception of Fig. 6 it is impossible to display single data points as such. Instead one should think of each pixel in Fig. 1 as representing information on whether or not it contains a data point. In Figs. 2 to 5 every pixel is given a particular shade of grey depending on the number of Hodge data sets giving rise to data points lying there; the greyscales are obviously different for different figures. Only in Fig. 6 single data points are visible. Here every pair  $(h^{1,1}, h^{1,3})$  that is realized by at least one weight system is indicated by a circle. This circle is filled in those rare cases in which a Hodge triple with negative Euler number exists (we discuss the scarcity of such points below).

The remaining figures give information on the frequencies of occurrences of specific values. The plots in Figs. 7 to 18 indicate the numbers of Hodge data sets in which a particular value of one of the Hodge numbers or  $\chi$  is taken, whereas the remaining plots indicate how many different weight systems give rise to the quantity in question. Perhaps the most notable feature of these plots is the distribution of possible values for the Euler characteristic  $\chi$ . Unless one zooms into the very left end of the distribution, as in Fig. 17 and Fig. 29, the plots appear to start at  $\chi = 0$ . The somewhat surprising scarcity and small values of negative Euler characteristics are consequences of

$$\chi = 4 + 2h^{1,1} - 4h^{1,2} + 2h^{1,3} + h^{2,2} = 6(8 + h^{1,1} - h^{1,2} + h^{1,3}) \quad (28)$$

(cf. formula (4)) which implies  $\chi < 0 \Leftrightarrow h^{1,2} > 8 + h^{1,1} + h^{1,3}$ , together with the small range of values of  $h^{1,2}$  compared to those of  $h^{1,1}$  and  $h^{1,3}$ . Structures



with a band-like appearance as in Figs. 15, 18, 27 and 30 are also related to (4) and (28): assuming that both  $h^{1,2}$  and  $h^{1,1} + h^{1,3}$  have a preference for being even,  $\chi/6 = 8 + h^{1,1} - h^{1,2} + h^{1,3}$  and  $h^{2,2}/2 = 22 + 2h^{1,1} - h^{1,2} + 2h^{1,3}$  will also tend to be even rather than odd; in Figs. 18 and 30 we can even see a preference for  $\chi/6$  to be a multiple of 4.

While our main focus here is on the weight systems that determine reflexive polytopes, one should not ignore the ones giving polytopes with the IP property that lack reflexivity. On the one hand they are indispensable ingredients in a full classification of reflexive polytopes. On the other hand polytopes of this type may well be interesting on their own. Originally reflexivity was singled out as the condition that leads to smooth Calabi–Yau hypersurfaces in toric varieties of dimension up to four [6]. If one does not insist on smoothness, which is not even guaranteed by reflexivity for polytope dimension  $d > 4$  anyway, the following setup becomes important. In a notation in which  $[\Delta]$  stands for  $\text{conv}(\Delta \cap M)$  (with an analogous definition for polytopes in  $N_{\mathbb{R}}$ ) a special role is played by IP polytopes that satisfy

$$\Delta = [\Delta] = [[\Delta^*]^*] \quad (29)$$

(the first condition  $\Delta = [\Delta]$  just means that  $\Delta$  is a lattice polytope). Such polytopes are called *almost reflexive* [27] or *pseudoreflexive* [28] and give rise to well-defined singular varieties of Calabi–Yau type.

We will now argue that our polytopes  $\Delta_{\mathbf{q}}$  satisfy condition (29). If we denote by  $\nabla_{\mathbf{q}}$  the simplex in  $N_{\text{coarsest}}$  determined by some weight system  $\mathbf{q}$  with the IP property, then  $\Delta_{\mathbf{q}} = [\nabla_{\mathbf{q}}^*] \subseteq \nabla_{\mathbf{q}}^*$ , hence  $\Delta_{\mathbf{q}}^* \supseteq \nabla_{\mathbf{q}}$ ; since  $\nabla_{\mathbf{q}}$  is a lattice polytope this implies  $[\Delta_{\mathbf{q}}^*] \supseteq \nabla_{\mathbf{q}}$  and therefore  $[[\Delta_{\mathbf{q}}^*]^*] \subseteq [\nabla_{\mathbf{q}}^*] = \Delta_{\mathbf{q}}$ . Conversely,  $[\Delta_{\mathbf{q}}^*] \subseteq \Delta_{\mathbf{q}}^*$  gives  $[\Delta_{\mathbf{q}}^*]^* \supseteq \Delta_{\mathbf{q}}$  which implies  $[[\Delta_{\mathbf{q}}^*]^*] \supseteq \Delta_{\mathbf{q}}$  because  $\Delta_{\mathbf{q}}$  is a lattice polytope. Therefore indeed  $[[\Delta_{\mathbf{q}}^*]^*] = \Delta_{\mathbf{q}}$ . This fits well with the fact that both the lattice polytope  $\nabla_{\mathbf{q}}$  and  $[\nabla_{\mathbf{q}}^*]$  are IP polytopes, which means that  $\nabla_{\mathbf{q}}$  is *almost pseudoreflexive* in the sense of Def. 3.6 and Prop. 3.4 of Ref. [28], whose Corollary 3.5 also implies that  $\Delta_{\mathbf{q}}$  satisfies condition (29).

**Acknowledgements:** The authors thank Victor Batyrev for email correspondence and Roman Schönbichler for helpful discussions. We are grateful to the Vienna Scientific Cluster for unbureaucratically providing computing time and in particular to Ernst Haunschmid for explanations on how to use these resources. F.S. has been supported by the Austrian Science Fund (FWF), projects P 27182-N27 and P 28751-N27.

## Appendix: Visualization of results

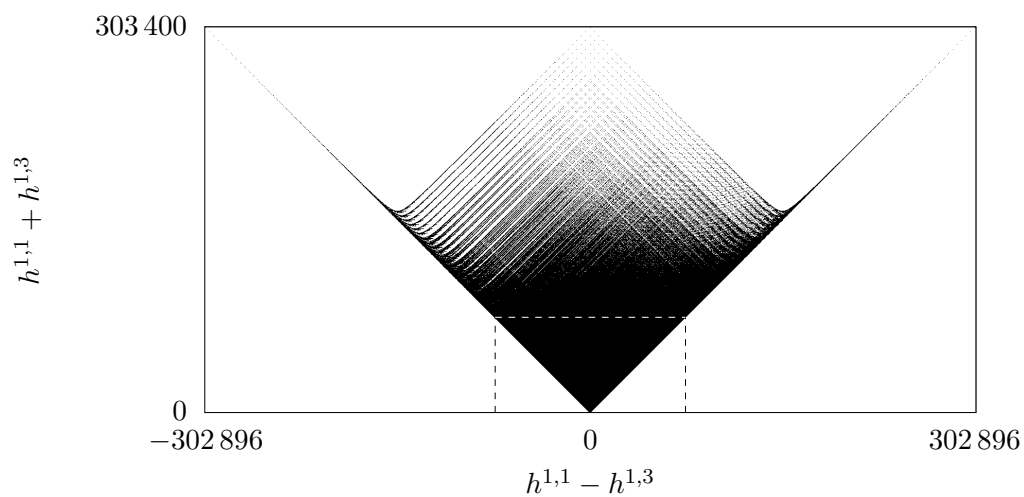


Figure 1: All values of  $(h^{1,1}, h^{1,3})$ ; the rectangle bounded by dashed lines indicates the range of Fig. 2.

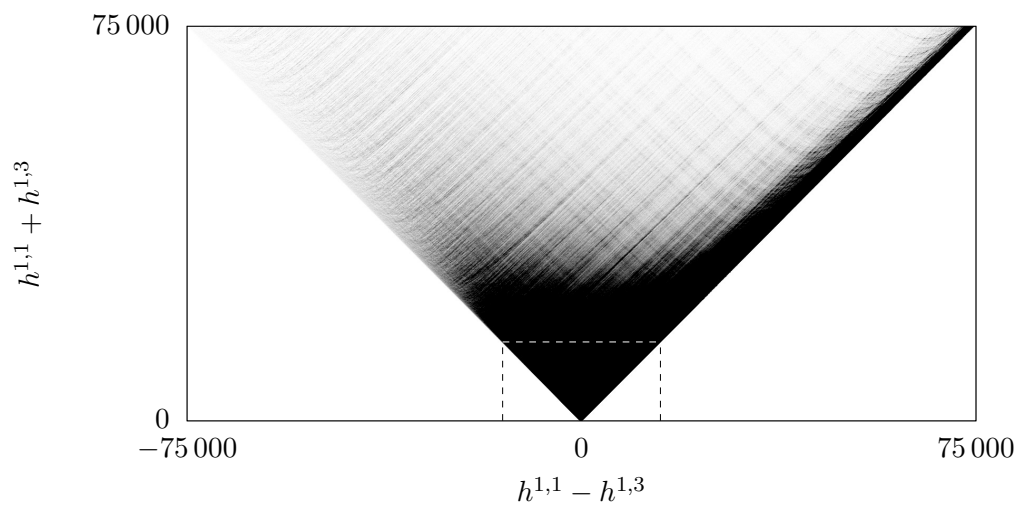


Figure 2:  $(h^{1,1}, h^{1,3})$  with  $h^{1,1} + h^{1,3} \leq 75\,000$ : greyscale indicates frequency; the rectangle bounded by dashed lines indicates the range of Fig. 3.

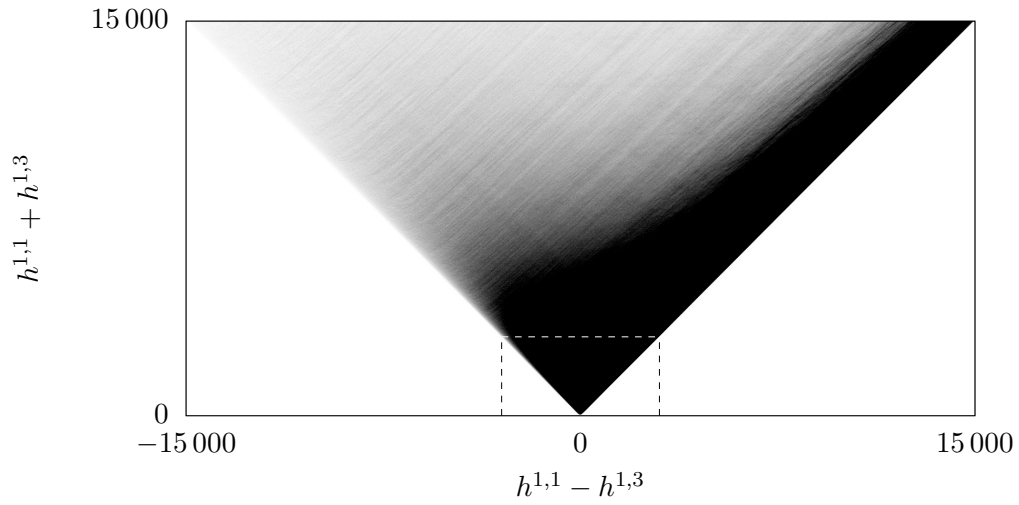


Figure 3:  $(h^{1,1}, h^{1,3})$  with  $h^{1,1} + h^{1,3} \leq 15000$ : greyscale indicates frequency; the rectangle bounded by dashed lines indicates the range of Fig. 4.

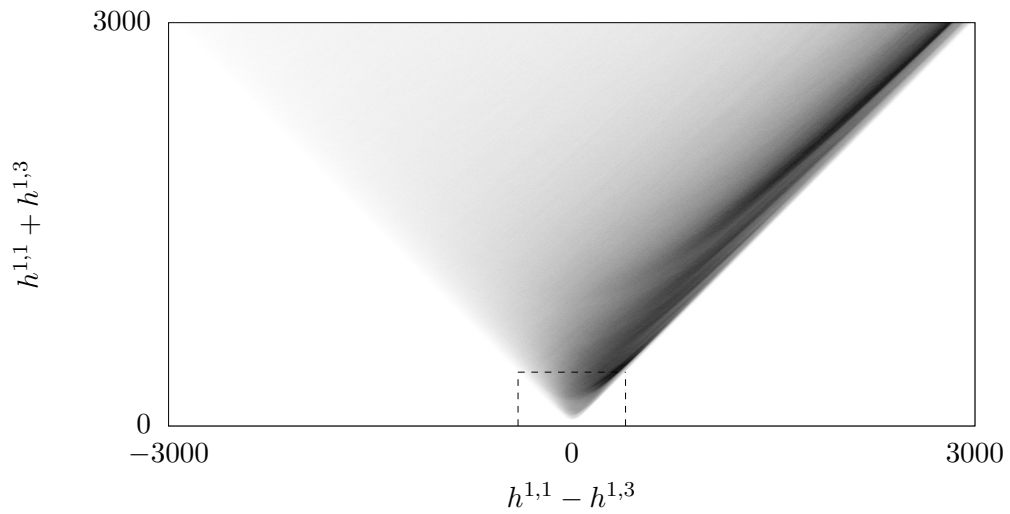


Figure 4:  $(h^{1,1}, h^{1,3})$  with  $h^{1,1} + h^{1,3} \leq 3000$ : greyscale indicates frequency; the rectangle bounded by dashed lines indicates the range of Fig. 5.

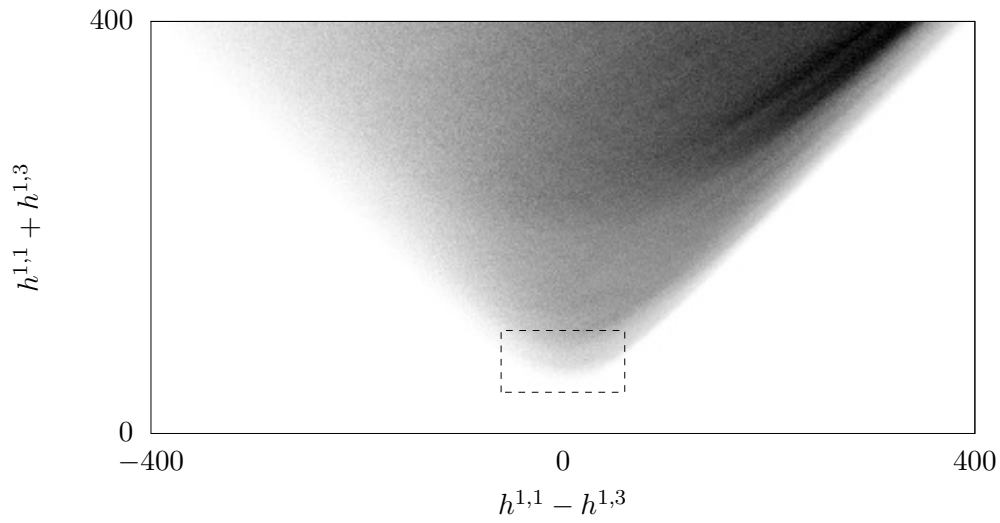


Figure 5:  $(h^{1,1}, h^{1,3})$  with  $h^{1,1} + h^{1,3} \leq 400$ : greyscale indicates frequency; the rectangle bounded by dashed lines indicates the range of Fig. 6.

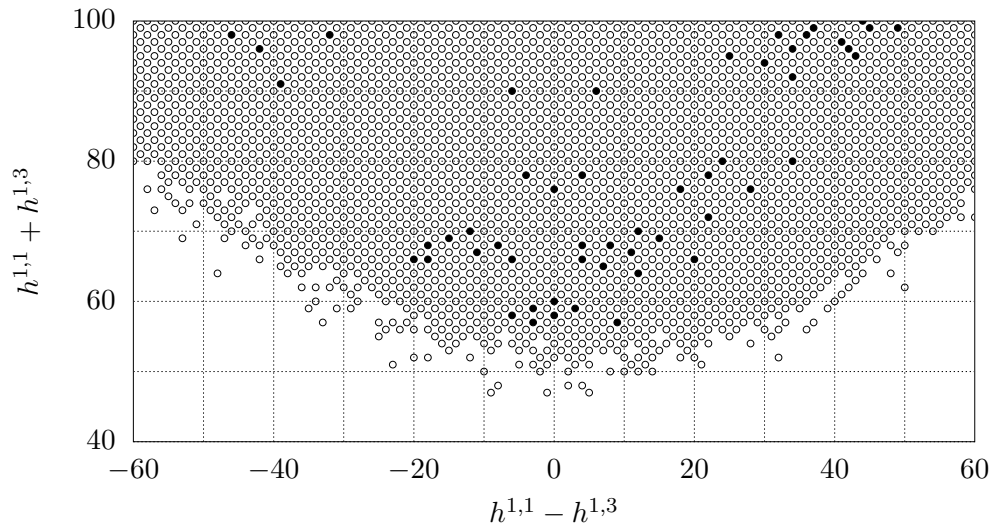


Figure 6: Small values of  $(h^{1,1}, h^{1,3})$ : solid circles indicate pairs admitting negative Euler characteristic.

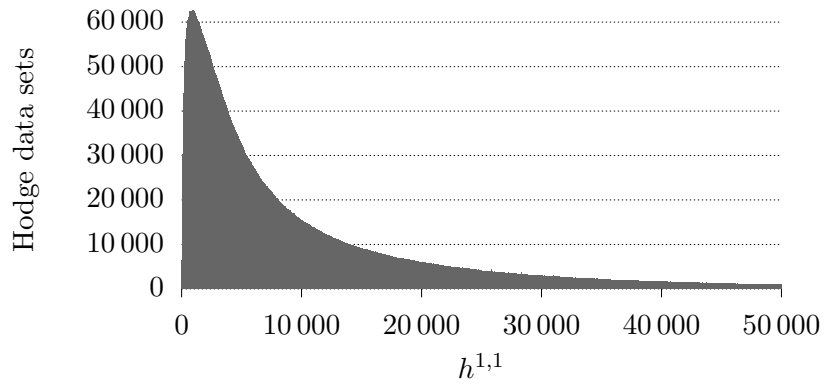


Figure 7: Numbers of Hodge data sets with a given value of  $h^{1,1}$

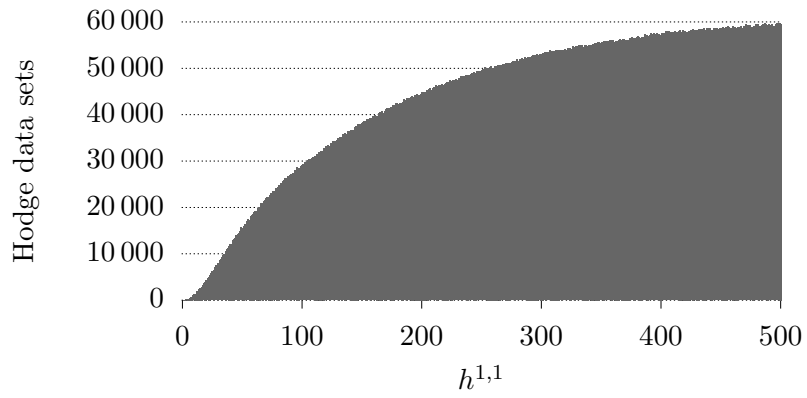


Figure 8: Numbers of Hodge data sets with a given value of  $h^{1,1}$

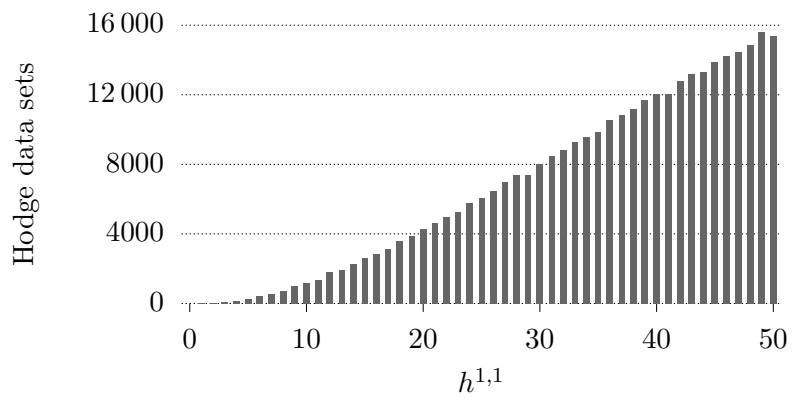


Figure 9: Numbers of Hodge data sets with a given value of  $h^{1,1}$

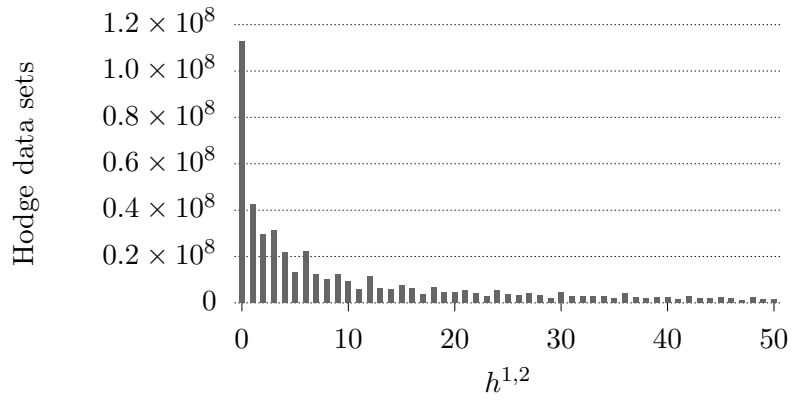


Figure 10: Numbers of Hodge data sets with a given value of  $h^{1,2}$

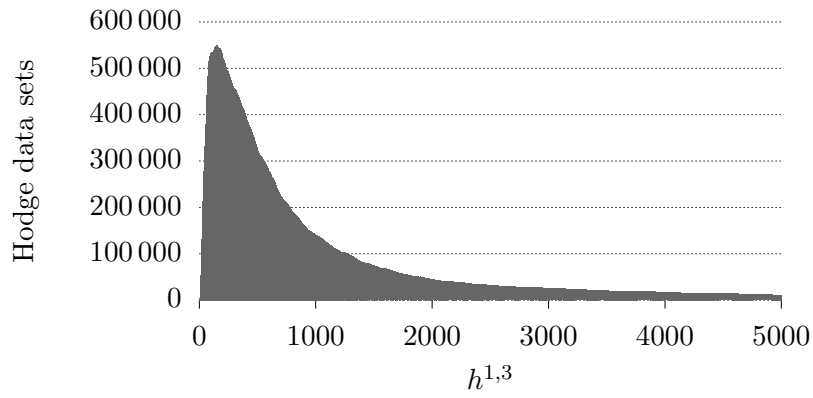


Figure 11: Numbers of Hodge data sets with a given value of  $h^{1,3}$

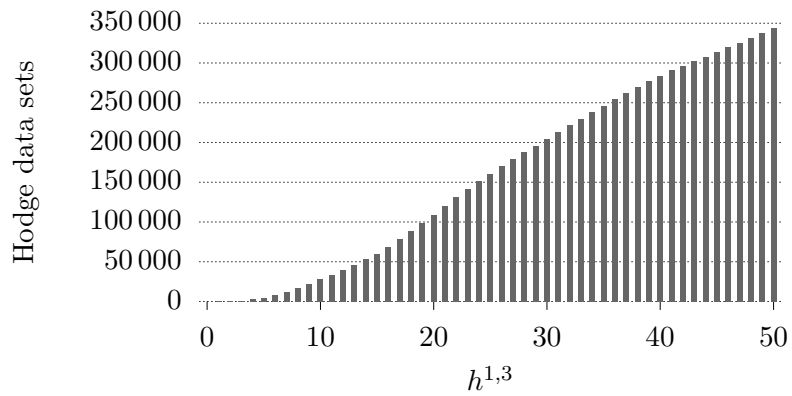


Figure 12: Numbers of Hodge data sets with a given value of  $h^{1,3}$

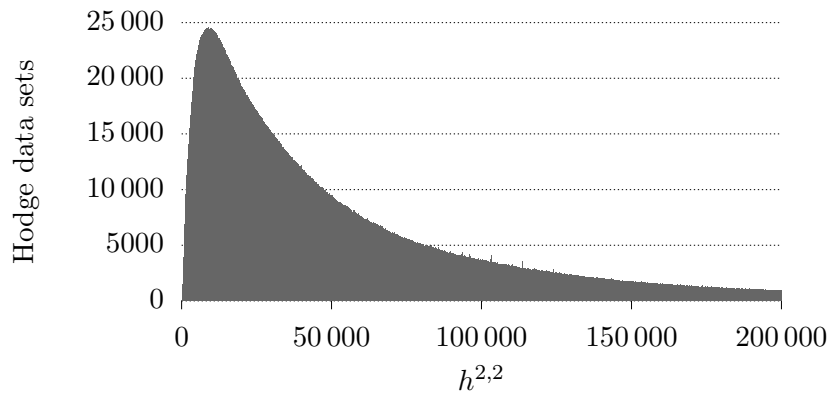


Figure 13: Numbers of Hodge data sets with a given value of  $h^{2,2}$

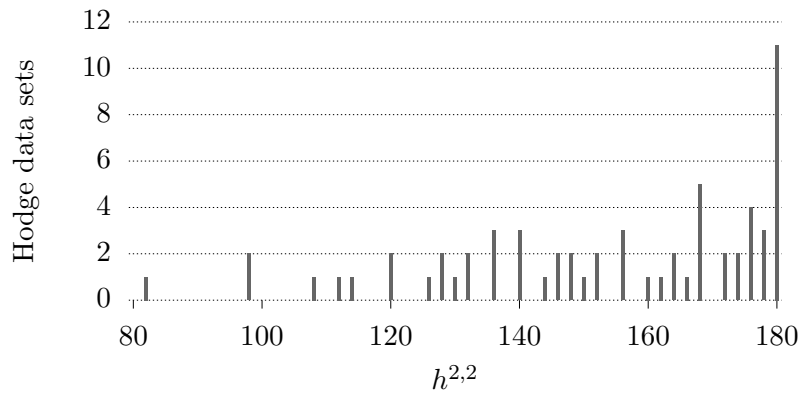


Figure 14: Numbers of Hodge data sets with a given value of  $h^{2,2}$

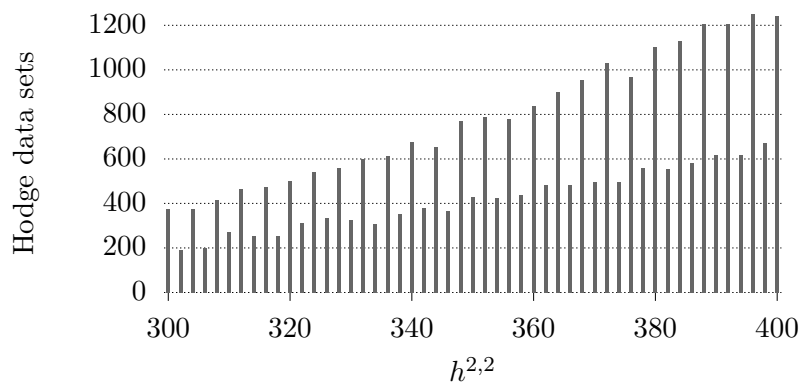


Figure 15: Numbers of Hodge data sets with a given value of  $h^{2,2}$

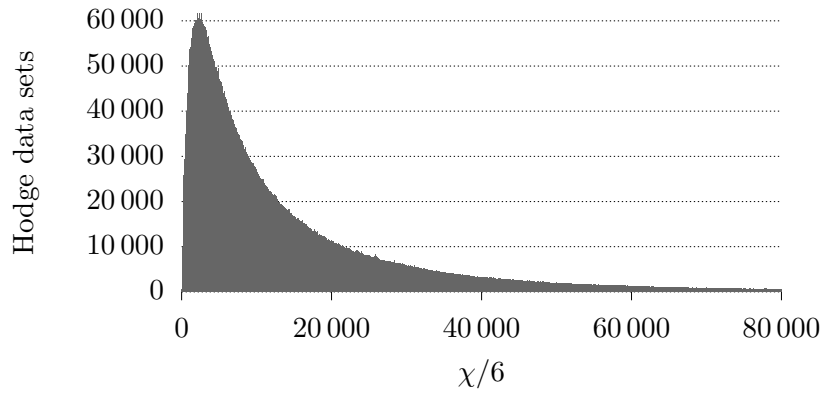


Figure 16: Numbers of Hodge data sets with a given value of  $\chi$

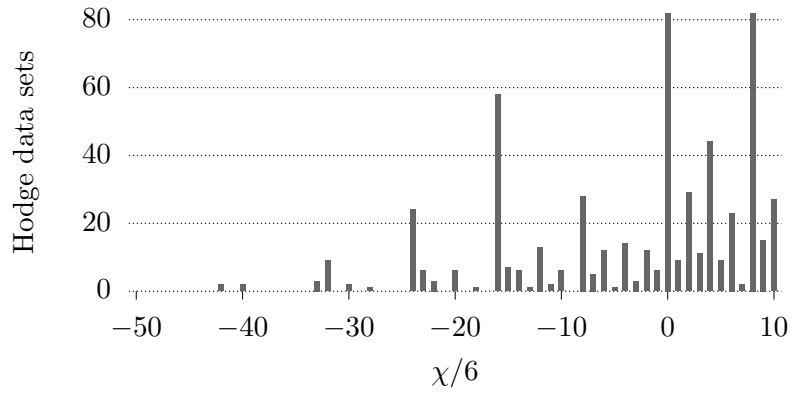


Figure 17: Numbers of Hodge data sets with a given value of  $\chi$

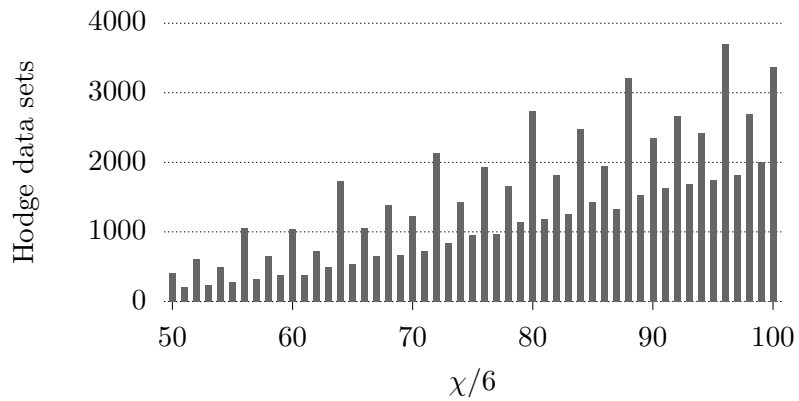


Figure 18: Numbers of Hodge data sets with a given value of  $\chi$



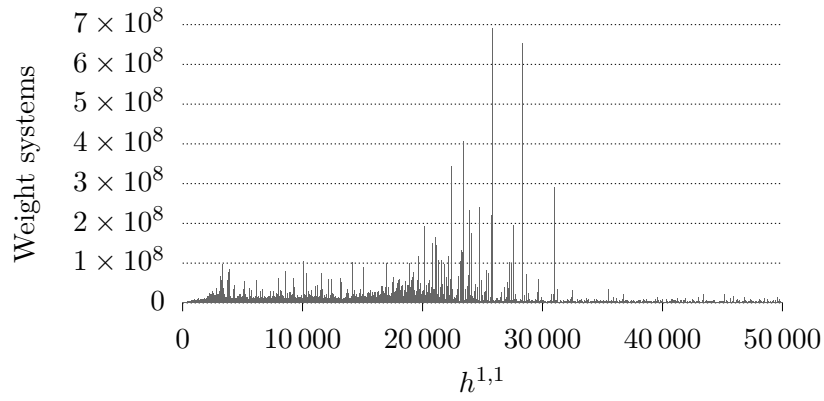


Figure 19: Numbers of weight systems leading to a given value of  $h^{1,1}$

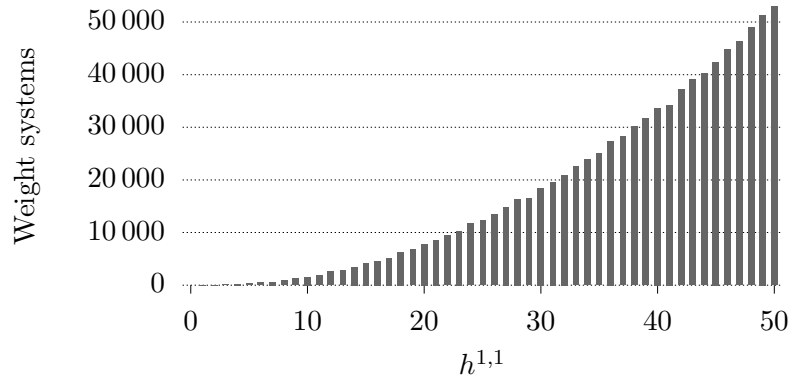


Figure 20: Numbers of weight systems leading to a given value of  $h^{1,1}$

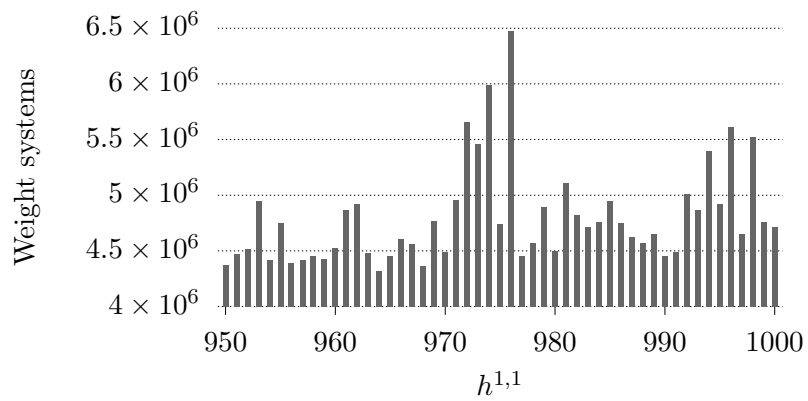


Figure 21: Numbers of weight systems leading to a given value of  $h^{1,1}$

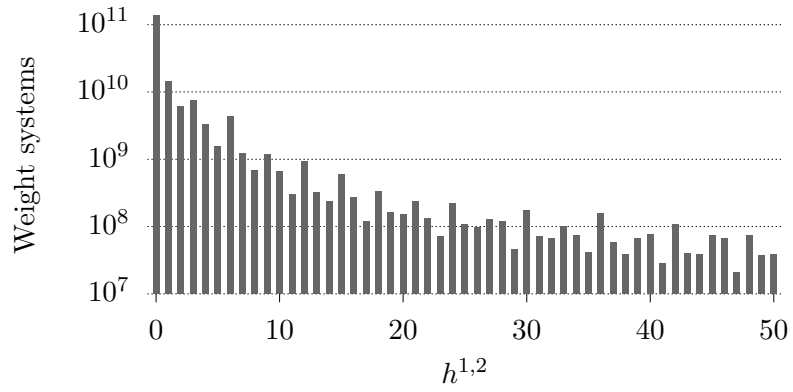


Figure 22: Numbers of weight systems leading to a given value of  $h^{1,2}$

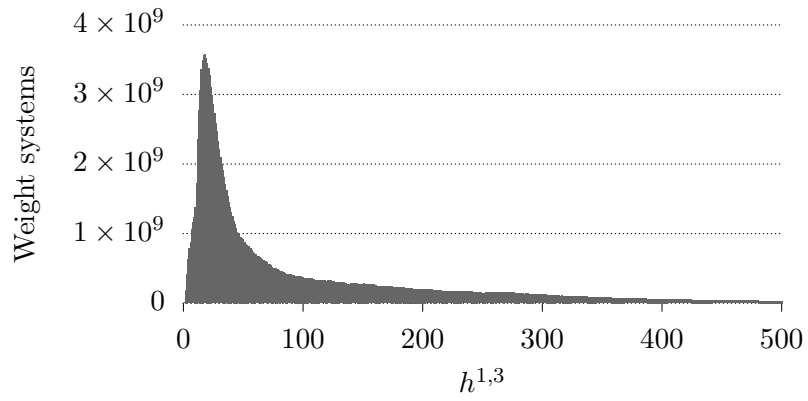


Figure 23: Numbers of weight systems leading to a given value of  $h^{1,3}$

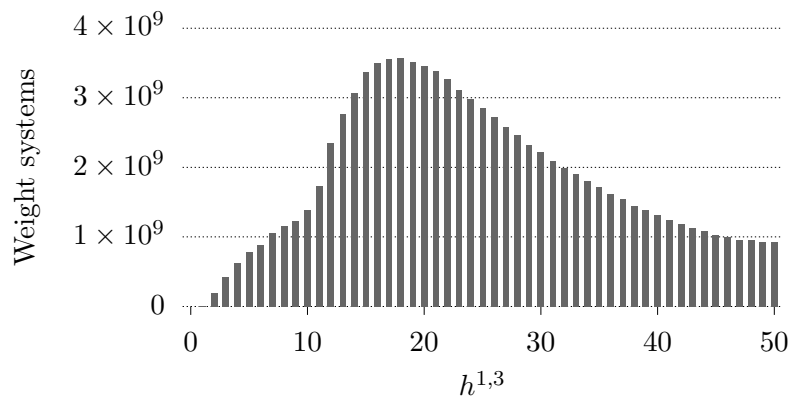


Figure 24: Numbers of weight systems leading to a given value of  $h^{1,3}$

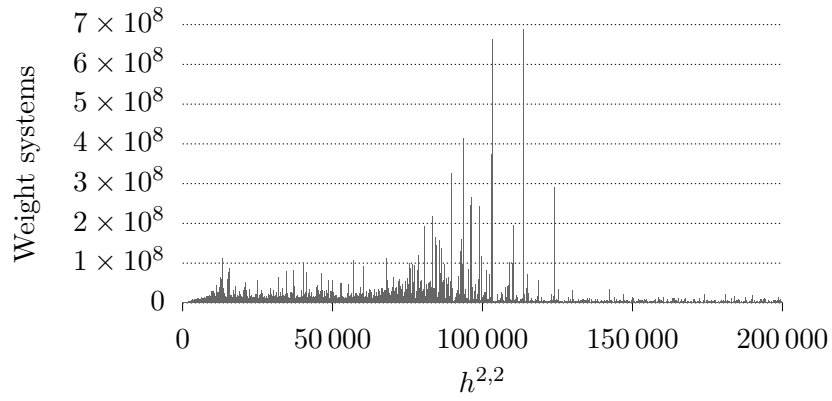


Figure 25: Numbers of weight systems leading to a given value of  $h^{2,2}$

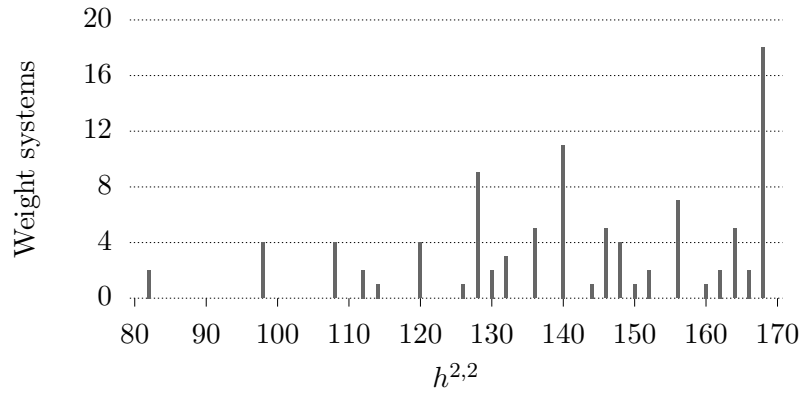


Figure 26: Numbers of weight systems leading to a given value of  $h^{2,2}$

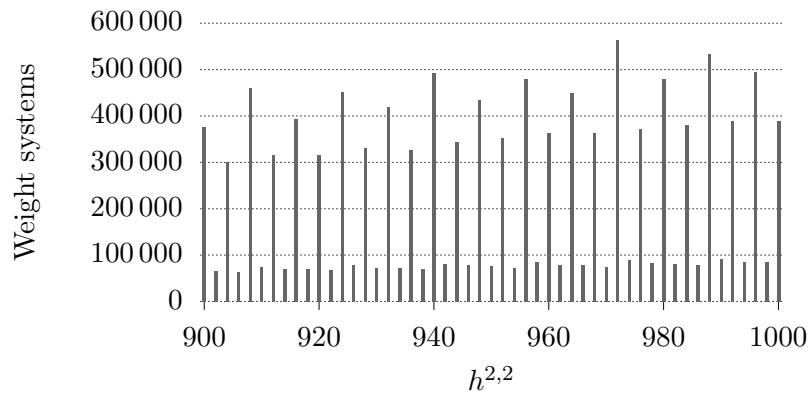


Figure 27: Numbers of weight systems leading to a given value of  $h^{2,2}$

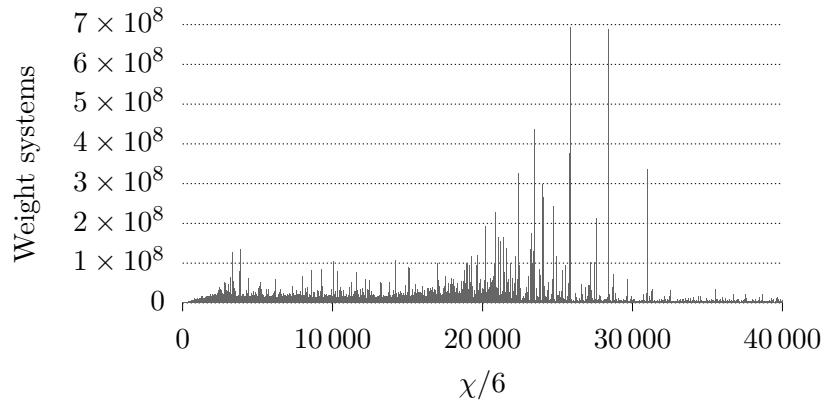


Figure 28: Numbers of weight systems leading to a given value of  $\chi$

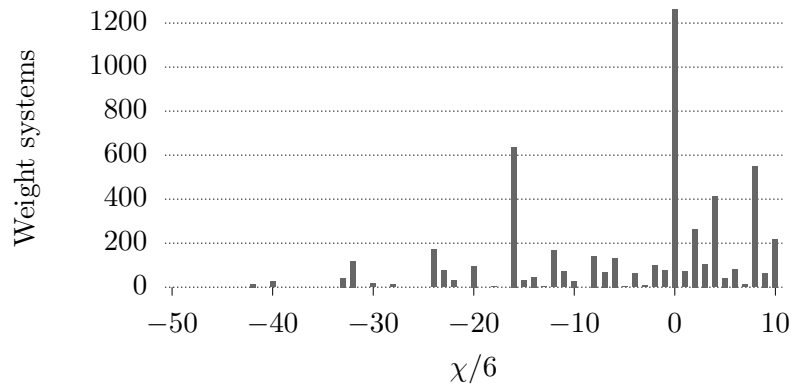


Figure 29: Numbers of weight systems leading to a given value of  $\chi$

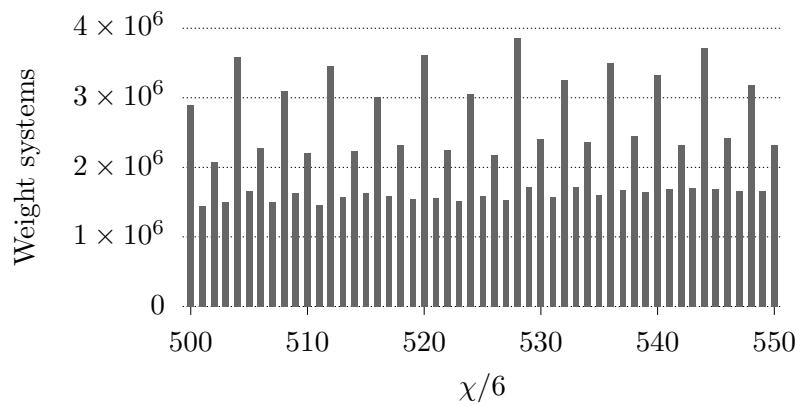


Figure 30: Numbers of weight systems leading to a given value of  $\chi$

## References

- [1] P. Candelas, G. T. Horowitz, A. Strominger, and E. Witten, “Vacuum Configurations for Superstrings,” *Nucl. Phys.* **B258** (1985) 46–74.
- [2] P. Candelas, A. M. Dale, C. A. Lutken, and R. Schimmrigk, “Complete Intersection Calabi-Yau Manifolds,” *Nucl. Phys.* **B298** (1988) 493.
- [3] A. Klemm and R. Schimmrigk, “Landau-Ginzburg string vacua,” *Nucl. Phys.* **B411** (1994) 559–583, [arXiv:hep-th/9204060 \[hep-th\]](#).
- [4] M. Kreuzer and H. Skarke, “No mirror symmetry in Landau-Ginzburg spectra!,” *Nucl. Phys.* **B388** (1992) 113–130, [arXiv:hep-th/9205004 \[hep-th\]](#).
- [5] M. Kreuzer and H. Skarke, “All Abelian symmetries of Landau-Ginzburg potentials,” *Nucl. Phys.* **B405** (1993) 305–325, [arXiv:hep-th/9211047 \[hep-th\]](#).
- [6] V. V. Batyrev, “Dual polyhedra and mirror symmetry for Calabi-Yau hypersurfaces in toric varieties,” *J. Alg. Geom.* **3** (1994) 493–545, [arXiv:alg-geom/9310003 \[alg-geom\]](#).
- [7] V. V. Batyrev and L. A. Borisov, “Dual Cones and Mirror Symmetry for Generalized Calabi-Yau Manifolds,” [arXiv:alg-geom/9402002](#).
- [8] E. Witten, “Phases of N=2 theories in two-dimensions,” *Nucl. Phys.* **B403** (1993) 159–222, [arXiv:hep-th/9301042 \[hep-th\]](#).
- [9] H. Skarke, “Weight systems for toric Calabi-Yau varieties and reflexivity of Newton polyhedra,” *Mod. Phys. Lett.* **A11** (1996) 1637–1652, [arXiv:alg-geom/9603007 \[alg-geom\]](#).
- [10] A. C. Avram, M. Kreuzer, M. Mandelberg, and H. Skarke, “The Web of Calabi-Yau hypersurfaces in toric varieties,” *Nucl. Phys.* **B505** (1997) 625–640, [arXiv:hep-th/9703003 \[hep-th\]](#).
- [11] M. Kreuzer and H. Skarke, “Complete classification of reflexive polyhedra in four-dimensions,” *Adv. Theor. Math. Phys.* **4** (2002) 1209–1230, [arXiv:hep-th/0002240 \[hep-th\]](#).
- [12] H. Skarke, “How to Classify Reflexive Gorenstein Cones,” in *Strings, gauge fields, and the geometry behind: The legacy of Maximilian Kreuzer*, A. Rebhan, L. Katzarkov, J. Knapp, R. Rashkov, and E. Scheidegger, eds., pp. 443–458. 2012. [arXiv:1204.1181 \[hep-th\]](#).

- [13] C. Vafa, “Evidence for F theory,” *Nucl. Phys.* **B469** (1996) 403–418, [arXiv:hep-th/9602022](#) [hep-th].
- [14] M. Lynker, R. Schimmrigk, and A. Wisskirchen, “Landau-Ginzburg vacua of string, M theory and F theory at  $c = 12$ ,” *Nucl. Phys.* **B550** (1999) 123–150, [arXiv:hep-th/9812195](#) [hep-th].
- [15] J. Gray, A. S. Haupt, and A. Lukas, “All Complete Intersection Calabi-Yau Four-Folds,” *JHEP* **07** (2013) 070, [arXiv:1303.1832](#) [hep-th].
- [16] M. Kreuzer and H. Skarke, “Classification of reflexive polyhedra in three-dimensions,” *Adv. Theor. Math. Phys.* **2** (1998) 853–871, [arXiv:hep-th/9805190](#) [hep-th].
- [17] V. V. Batyrev and D. I. Dais, “Strong McKay correspondence, string theoretic Hodge numbers and mirror symmetry,” [arXiv:alg-geom/9410001](#) [alg-geom].
- [18] M. Kreuzer and H. Skarke, “On the classification of reflexive polyhedra,” *Commun. Math. Phys.* **185** (1997) 495–508, [arXiv:hep-th/9512204](#) [hep-th].
- [19] M. Kreuzer and H. Skarke, “Reflexive polyhedra, weights and toric Calabi-Yau fibrations,” *Rev. Math. Phys.* **14** (2002) 343–374, [arXiv:math/0001106](#) [math-ag].
- [20] M. Kreuzer and H. Skarke, “PALP: A Package for analyzing lattice polytopes with applications to toric geometry,” *Comput. Phys. Commun.* **157** (2004) 87–106, [arXiv:math/0204356](#) [math.NA].
- [21] A. P. Braun, J. Knapp, E. Scheidegger, H. Skarke, and N.-O. Walliser, “PALP - a User Manual,” in *Strings, gauge fields, and the geometry behind: The legacy of Maximilian Kreuzer*, A. Rebban, L. Katzarkov, J. Knapp, R. Rashkov, and E. Scheidegger, eds., pp. 461–550. 2012. [arXiv:1205.4147](#) [math.AG].
- [22] M. Kreuzer and H. Skarke, “Calabi-Yau data.” <http://hep.itp.tuwien.ac.at/~kreuzer/CY/>.
- [23] M. Kreuzer and H. Skarke, “Calabi-Yau four folds and toric fibrations,” *J. Geom. Phys.* **26** (1998) 272–290, [arXiv:hep-th/9701175](#) [hep-th].
- [24] P. Candelas, A. Constantin, and H. Skarke, “An Abundance of K3 Fibrations from Polyhedra with Interchangeable Parts,” *Commun. Math. Phys.* **324** (2013) 937–959, [arXiv:1207.4792](#) [hep-th].

- [25] P. Candelas and A. Font, “Duality between the webs of heterotic and type II vacua,” *Nucl. Phys.* **B511** (1998) 295–325, [arXiv:hep-th/9603170](#) [[hep-th](#)].
- [26] P. Candelas and H. Skarke, “F theory, SO(32) and toric geometry,” *Phys. Lett.* **B413** (1997) 63–69, [arXiv:hep-th/9706226](#) [[hep-th](#)].
- [27] A. R. Mavlyutov, “Mirror Symmetry for Calabi-Yau complete intersections in Fano toric varieties,” [arXiv:1103.2093](#) [[math.AG](#)].
- [28] V. Batyrev, “The stringy Euler number of Calabi-Yau hypersurfaces in toric varieties and the Mavlyutov duality,” [arXiv:1707.02602](#) [[math.AG](#)].